Hindawi
Journal of Control Science and Engineering
Volume 2018, Article ID 2738362, 9 pages
https://doi.org/10.1155/2018/2738362

Research Article

Wide-Area Damping Controller Design Based on the Frequency Domain Self-Excitation Method

Lei Gao,[1,2] Yanchao Ma,[3] Yonghui Nie,[2] Shiyun Xu,[1] Xiaojie Chu,[1] and Long Peng[1]

[1]*China Electric Power Research Institute, Beijing 100192, China*
[2]*Northeast Electric Power University, Jilin 132012, Jilin Province, China*
[3]*State Grid Liaoning Power Co., Ltd., Yingkou Power Supply Company, Yingkou 115000, China*

Correspondence should be addressed to Shiyun Xu; xushiyun@epri.sgcc.com.cn

Received 9 May 2018; Accepted 16 August 2018; Published 13 September 2018

Academic Editor: Cui-Qin Ma

Copyright © 2018 Lei Gao et al. This is an open access article distributed under the Creative Commons Attribution License, which permits unrestricted use, distribution, and reproduction in any medium, provided the original work is properly cited.

In this paper, a wide-area DC damping controller design method is proposed to damp the weak interarea oscillation modes. First, the low-order power system control model identification method is proposed based on the frequency domain self-excitation method to obtain the dominant modes and other related information. In what follows, the identified model is transformed into a low-order state space equation. By comparing the geometric metrics of different schemes, the various input signals and installation locations of the controller are selected. Furthermore, the damping controller parameter calculation is realized based on the self-excitation frequency domain identification method, which does not depend on the detailed model of the system. The design process is simple and it is easy to apply in the practical engineering of large-scale complex power grids. The applicability and effectiveness of the proposed controller design method are demonstrated through simulations of a two-area four-generator power system.

1. Introduction

The AC/DC interconnected power grid can transmit large capacity of power from the remote power basis to the load centers through communication networks. It plays an extremely important role in the energy allocation in China. Since the AC and DC transmission systems are generally coupled with each other, however, disturbances that occur in both the AC and the DC sides may trigger weakly damped low frequency oscillations. If the oscillations are of the interarea type, a large number of generators will participate in and the interconnected power grid will confront severe operational risk [1, 2].

However, due to the deficiency in observability, traditional power system stabilizers (PSS) which use local signals as inputs may fail to damp out the interarea oscillation and maintain system stability. To overcome the shortcoming of traditional PSS, wide-area damping controllers with remote signals obtained from wide-area measurement system (WAMS) have become a better choice in suppressing low frequency oscillation [3–5]. Since DC systems have fast response characteristics, it can effectively improve the stability of the system once faults have occurred in the AC system, and the DC damping control [6–9] that can suppress the interarea low frequency oscillation of AC/DC hybrid system has attracted the attention of researchers.

During the wide-area damping controller design, it is important to choose feedback control signal and installation location. The residue method [10, 11] is widely used for feedback signal selection, but it can only compare the same type of signals. For different types of signals, such as generator speed, line transmission power, and bus voltage, the amplitude of the above-mentioned residual value will not be accurate due to the ratio problem. In [12], a relative gain array (RGA) method is proposed. Although this method reduces the mutual influence among multiple controllers, it has the same disadvantages as the residual method. Other methods, such as the Hankel singular value (HSV) [13], the singular value decomposition (SVD) [14], and the minimum singular values (MSV) [15], have also been proposed to calculate the corresponding observability and controllability indices, but it becomes much more complicated to calculate for practical large-scale power systems. On the other hand, most of the existing damping control design methods require the precise

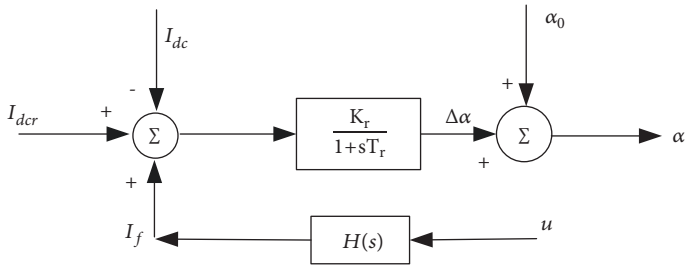

Figure 1: Rectifier current regulator.

system model through linearizing it around an equilibrium point. This may lead to the modeling error due to information incompleteness.

In this paper, the low frequency oscillation of an AC/DC hybrid system is damped by installing a wide-area damping controller in the DC system. Based on the above considerations, the improved geometric lateral index [11, 16] based on the frequency domain excitation identification theory is proposed to solve the wide-area DC supplementary damping control signal selection in AC/DC hybrid systems. This method can effectively solve the problem that different types of input signals have different amplitude ratios and can avoid solving the huge state matrix as well. Moreover, the method based on the self-excitation frequency domain identification is further utilized to configure the DC damping controller, which does not depend on the detailed model of the system. The design process is simple, and it is easy to use in the practical engineering of the complex large power grid. At the end of this study, the AC/DC hybrid system is taken as an example to demonstrate the effectiveness of the proposed controller design method.

2. Problem Formulation

2.1. DC Damping Controller. The DC damping control is a kind of small signal modulation, and the basic principle is to add a supplementary damping controller in the DC main control loop. The controller is usually installed at the rectifier side. In this regard, the power of the DC transmission line is adjusted by tuning the extinction angle α to damp the system oscillation.

The control block diagram is shown in Figure 1. By adding the DC additional control output I_f and the reference current input I_{dcr} to the current control of the inverter can improve the damping of the system. The dynamic equation of the linearized regulator is given as

$$\begin{aligned} \dot{\alpha} &= \frac{K_r}{T_r}\left(I_{dcr} - I_{dc} + I_f\right) - \frac{\alpha}{T_r} \\ \dot{I}_{dc} &= \frac{1}{T_{dc}}\left(-I_{dc} + I_{dcr} + I_f\right) \end{aligned} \tag{1}$$

The supplementary wide-area damping controller transfer function is in the following form:

$$H(s) = \frac{K}{1+sT_1} \cdot \frac{sT_W}{1+sT_W} \cdot \left[\frac{1+sT_2}{1+sT_3}\right]^m \tag{2}$$

where T_{dc}, T_r, T_1, T_2, T_3, T_W are the time constants, K_r and K are the controller proportional coefficient, I_{dc} is the DC current, and u is the feedback signal, which can be chosen as the generator speed deviation, the bus phase difference or any bus voltage, power, and so on.

In this study, the selected feedback signal is processed by the damping controller to the input of the current regulator in the DC main control system, based on the principle of DC damping control. The extinction angle α is maintained within the normal range ($\alpha_{\min} < \alpha < \alpha_{\max}$). In order to select the best alternative signal, the indicators defined by the improved geometric index can be calculated. In this regard, the designed damping controller can damp system oscillation.

2.2. System Model Analysis. By linearizing around the stable equilibrium point, the AC/DC hybrid power system equation can be given as

$$\begin{aligned} \Delta\dot{x} &= A\Delta x + B\Delta u \\ \Delta y &= C\Delta x \end{aligned} \tag{3}$$

where A is an $n \times n$ state matrix, B is an $n \times p$ input matrix, and C is a $q \times n$ output matrix.

For power system with n generators, only part of the oscillation mode of the generator rotor is concerned, and the number of oscillating modes in which any one generator is significantly involved is generally 2~3. Based on this consideration, the state equation of the ith generator can be set as

$$\begin{bmatrix} \Delta\dot{\delta} \\ \Delta\dot{\omega} \end{bmatrix} = \begin{bmatrix} 0 & I \\ -M^{-1}K(s) & -M^{-1}D(s) \end{bmatrix} \cdot \begin{bmatrix} \Delta\delta \\ \Delta\omega \end{bmatrix} \tag{4}$$

where $K(s)$ is the synchronization torque coefficient, $D(s)$ is the damping torque coefficient, and M is the diagonal matrix composed by the corresponding elements of the generator.

It can be seen from Figure 2 that if there is no external disturbance T_x, the differential equation of the corresponding equivalent system can be derived as

$$M(s)\Delta\ddot{\delta} + D(s)\Delta\dot{\delta} + K(s)\Delta\delta = 0 \tag{5}$$

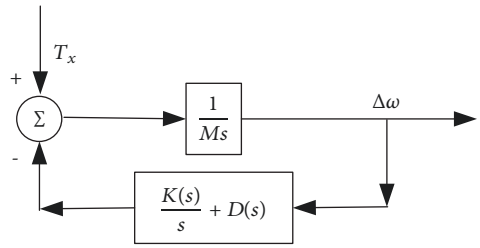

Figure 2: Equivalent system.

Assume that the eigenvalue of (5) is $\lambda_i = \sigma_i \pm j\omega_i$, then

$$\left(M\Delta\ddot{\delta} + D(s)\Delta\dot{\delta} + K(s)\Delta\delta\right)\Big|_{\lambda_i} \stackrel{\text{def}}{=} T_x \longrightarrow 0 \tag{6}$$

In order to calculate the electromechanical mode associated with system oscillation, the self-excited method [17] is utilized by deriving the eigenvalue of (6) through the Newton iteration method. However, the application of the traditional self-excited method is not only sensitive to the initial value but also easily leads to the loss of roots. In this regard, this paper proposes a frequency domain self-excited identification method, which is applied to choose controller inputs. This method avoids the problems of traditional self-excited method, which is described in detail in the following section.

3. Wide-Area DC Damping Controller Design

Generally speaking, the steps in designing a wide-area controller include wide-area signal selection, system reduction, controller design, and validation of the design by numerical simulations. Each of the above steps is briefly described in the following subsections.

3.1. Observable and Controllable Quantitative Index. In order to choose the feedback signal and the installation location of the wide-area damping controller, it is necessary to establish a unified index for the calculation of different types of signals or control points. The quantization index of the observability and controllability of the system based on the improving geometric lateral index can solve the defects of the different types of signals, which is described as follows.

For system (3), by denoting a new state variable $\Delta x = Wz$, the oscillation characteristics of the system can be decoupled and the system with a diagonal state matrix can be derived as

$$\begin{aligned} \dot{z} &= \Lambda z + B'\Delta u \\ \Delta y &= C'z + D\Delta u, \end{aligned} \tag{7}$$

where W is the modal matrix of A, $\Lambda = \text{diag}\{\lambda_i\}$, $B' = W^{-1}B = N^T B$, $C' = CW$, W_i is the right eigenvector corresponding to λ_i, and N_i is the left eigenvector corresponding to λ_i.

The observability index of the ith modal of the system is given as

$$g_{oj}(i) = \cos\left(\alpha\left(W_i, c_j\right)\right) = \frac{\left|c_j W_i\right|}{\left\|W_i\right\| \left\|c_j\right\|} \tag{8}$$

while the controllability index is defined by

$$g_{ck}(i) = \cos\left(\theta\left(N_i, b_k\right)\right) = \frac{\left|b_k^T N_i\right|}{\left\|N_i\right\| \left\|b_k\right\|} \tag{9}$$

where $|\cdot|$ and $\|\cdot\|$, respectively, represent the modulo and Euclidean norm, c_j is the jth line of the matrix C, b_k is the kth column of the matrix B, $\alpha(W_i, c_j)$ is the angle between the output phasor c_j and the right eigenvector W_i, and $\theta(N_i, b_k)$ is the angle between the output phasor b_k and the left eigenvector N_i.

Thus, the comprehensive index corresponding to the ith modal is given by

$$\begin{aligned} g_{coi}(k, j) &= g_{oj}(i)\, g_{ck}(i) \\ &= \cos\left(\alpha\left(W_i, c_j\right)\right)\cos\left(\theta\left(N_i, b_k\right)\right) \end{aligned} \tag{10}$$

Quantitative analysis and comparison of the observability and controllability of different types of alternative signals can be realized by the calculation of the above-mentioned indices. However, in the practical power system, it is difficult to obtain the accurate full-order system model. Based on this consideration, this study carries out power system model identification according to the frequency domain self-excited method, and then the low-order system can be utilized to approximate the original system, which greatly reduces the calculation complicatedness and improves the calculation effectiveness.

3.2. Control Loop Selection. The feedback signals and installation locations selection are the basis for controller design of wide-area damping controller. In this subsection, a new method to select the feedback signal of wide-area damping controller is proposed by combining the basic principle of self-excitation and the method of frequency domain identification.

Based on the basic principle of the self-excited method, it can be derived from (6) that

$$T_x + \frac{dT_x}{ds}\left(\Delta\lambda_i\right) = 0 \tag{11}$$

By analyzing (11), the following necessary conditions are obtained:

$$\begin{aligned} T_x &\longrightarrow 0 \\ \frac{dT_x}{ds} &\longrightarrow 0 \end{aligned} \tag{12}$$

However, since the traditional self-excitation method iteratively solves the eigenvalue of (6) by Newton's method, it may lead to the incompleteness of electromechanical modes.

Therefore, the method proposed in this paper utilizes the frequency domain method to identify the transfer function of the system and then solve the relevant mode information to avoid the above-mentioned problems.

By carrying out the Laplace transform of (6) and (12), the system transfer function can be derived as

$$G(s) = \frac{\Delta\delta(s)}{\Delta T_x(s)} = \frac{s}{M(s)s^2 + D(s)s + K(s)} \tag{13}$$

If a more accurate model of the generator is considered, such as taking the excitation system model into account, (9) still holds, but the order will increase. In this case, $G(s)$ can be expressed as follows:

$$\begin{aligned} G(s) &= \frac{\Delta\delta_i(s)}{\Delta T_{xi}(s)} = K\frac{(s-z_{j1})(s-z_{j2})\cdots(s-z_{ji})}{(s-p_1)(s-p_2)\cdots(s-p_k)} \\ &= \frac{R_{j1}}{s-p_1} + \frac{R_{j2}}{s-p_2} + \cdots \frac{R_{jk}}{s-p_k} \end{aligned} \tag{14}$$

It can be analyzed from (6) and (12) that if the frequency of T_x is equal to the oscillation frequency of the system, only the torque with the amplitude close to zero can stimulate the large response of the oscillation frequency. Assume that T_x can increase the oscillation frequency to $\lambda\omega$, if different generators are selected as the "excitation point", then $G(\lambda_i\omega)$ can be expressed as

$$\begin{aligned} G(\lambda_i\omega) &= \frac{\Delta\delta_i(\lambda_i\omega)}{\Delta T_{xi}(\lambda_i\omega)} \\ &= \frac{R_{j1}}{\lambda_i\omega - p_1} + \frac{R_{j2}}{\lambda_i\omega - p_2} + \cdots \frac{R_{jk}}{\lambda_i\omega - p_k} \end{aligned} \tag{15}$$

Although the "excitation point" varies, the system inter-area oscillation mode keeps the same, where a pair of conjugate poles represents an oscillation mode. Let $\lambda_i = \sigma_i \pm j\omega_i$, then it can be used to calculate the system oscillation frequency and damping ratio.

Once the oscillation mode is determined, the index calculation of the candidate signal should be carried out, when it is necessary to transform the system into the state space form and $G(s)$ can be written as

$$G(s) = \frac{Y(s)}{U(s)} = \frac{b_m s^m + b_{m-1}s^{m-1} + \cdots + b_0}{s^n + a_{n-1}s^{n-1} + \cdots + a_0} \tag{16}$$

In this regard, the state space expression of the system can be derived as

$$\begin{aligned} \Delta\dot{x} &= E\Delta x + F\Delta u \\ \Delta y &= G\Delta x + H\Delta u \end{aligned} \tag{17}$$

where $E = \begin{bmatrix} 0 & I_{n-1} \\ A_0 & A_{n-1} \end{bmatrix}$ is the equivalent matrix of matrix A in (3), which contains the main mode of the original system. $F = [0 \ \cdots \ 1]^T$ and I are the corresponding control matrix and substantial matrix, respectively. $G = B_n - A_n b_n$, $H = b_n$. Equation (17) is the state space model derived by the frequency domain self-exited method.

The state space equation identified by the frequency domain excitation method preserves the main mode of operation of the system. Therefore, (17) can be used to substitute the original system to calculate the quantization index of the observability and controllability of the system.

The new method of selecting feedback signal of wide-area damping controller based on the self-excited frequency domain identification method proposed in this paper can be used in engineering application of large-scale power system without obtaining the full-state model of the system, and the calculation and operation are convenient, which is suitable for the engineering application of large power system.

3.3. Wide-Area Coordinated Controller Design. Once the state space equation is identified by the self-excited frequency domain identification, by carrying out the Laplace transform on (13), the transfer function between the input variable $\Delta\boldsymbol{U}_1$ and the output variable $\Delta\boldsymbol{Y}_1$ can be obtained as

$$G(s) = \frac{\Delta U_1(s)}{\Delta Y_1(s)} = G(sI - E)^{-1}F + H \tag{18}$$

Suppose dominant oscillation modes for (18) are $\lambda_{1,2} = \delta \pm j\omega$, and the desired damping ratio after adding damping controller is ξ. Substituting $s = j\omega_d = j\sqrt{1-\xi^2}\omega$ into (18) derives

$$G(j\omega_d) = \left.\frac{\Delta U_1(s)}{\Delta Y_1(s)}\right|_{s=j\omega_d} = G\angle\phi \tag{19}$$

where G and ϕ are the amplitude and phase of $G(s)$ at $s = j\omega_d$, respectively.

The lead lag link parameters of the wide-area DC damping controller (2) can be calculated by

$$\begin{aligned} \phi_x &= 180 - \phi \\ \alpha &= \frac{1+\sin\phi_x}{1-\sin\phi_x} \\ T_1 &= \frac{\sqrt{\alpha}}{\omega} \\ T_2 &= \frac{T_1}{\alpha} \end{aligned} \tag{20}$$

In order to prevent the damping controller from outputting a constant deviation voltage, the design principle is that, in the frequency range where damping controllers provide damping, no obvious phase displacement should be introduced in the isolating links. The typical value is chosen as 1~10s, and in this study, it is set to be 5s.

The advantage of the above wide-area DC damping controller parameter design based on the self-excited method is that it does not rely on the detailed model of the system, the design process is simple, the derived parameters are stable, and it is applicable to utilize in the practical complex large-scale power grid.

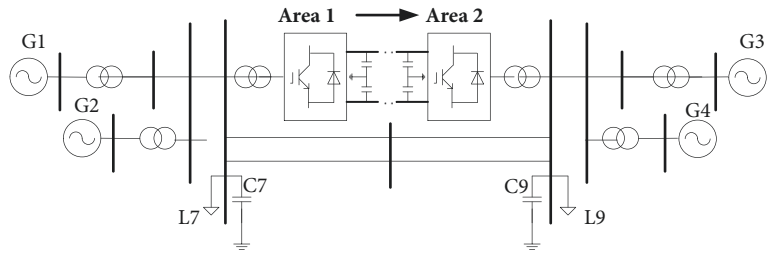

Figure 3: Two-area four-generator AC/DC hybrid system.

Table 1: Interarea oscillation frequency and damping ratio without control.

Operation mode	eigenvalue	frequency	Damping ratio
P=150MW	-0.1462+3.2683i	0.5202	0.0447
P=200MW	-0.1301+3.8321i	0.6099	0.0339
P=300MW	-0.2942+3.5092i	0.5585	0.0835

3.4. Wide-Area Damping Control Design Process. The basic steps of the selection of the feedback signal and the installation location of the wide-area damping controller based on the self-excited frequency domain identification method are as follows:

Step 1. Identify the low-order system based on the frequency domain self-excited method, and calculate the corresponding interarea oscillation modes $\lambda_{1,2} = \delta \pm j\omega$ and the oscillation frequency ω.

Step 2. Select different feedback signals and installation locations of the n groups of controllers, and then the system is able to be operated under the steady state with the open loop operation of the controller. The disturbance test for group i ($0<i<n$) is carried out, and for the disturbance $u_i(t)$ that does not destroy the stability of the original system, record the output response data $y_i(t)$.

Step 3. Extract the variation data $\Delta u_i(t)$ and $\Delta y_i(t)$ of $u_i(t)$ and $y_i(t)$ in the common cycle. Carry out the discrete Fourier transform, respectively, and obtain the varying phasors $\Delta u_i(j\omega)$ and $\Delta y_i(j\omega)$ corresponding to different frequency values, where $i = 1, 2, \ldots, n$, $0 \le j\omega \le 2\pi$.

Step 4. The self-excited method is applied to identify the phasor data $\Delta u_i(j\omega)$ and $\Delta y_i(j\omega)$, and the corresponding transfer function $G_i(s)$ is fitted. Transform the transfer function into the state space form and obtain the corresponding system matrices A_i, B_i, C_i, D_i.

Step 5. Apply the geometric measure index method to calculate each index, which is used as the reference for the input signal of the comparison controller. Based on the above method, that best feedback signal and installation location are determined.

Step 6. Based on the state space equation and the dominant modes, identify the information such as the phase Φ and the oscillation mode ω that are required by controller design. Calculate the controller time constants T_i, $i = 1, 2, \ldots, 4$ by (20).

Step 7. Adjust the controller gain K_i to verify the damping effect, and the operation parameters of the wide-area DC damping controller are finally determined.

4. Case Study

Taking the two-area four-generator AC/DC hybrid system shown in Figure 3 as an example, the detailed model is built with MATLAB and verified by simulation. The specific parameters are taken from literature [18]. The wide-area damping controller is installed in the rectifier of the DC part. The optional input signals of the wide-area damping controller are the rotor speed difference of generator 1 (G1) and generator 3 (G3), the active power of the AC tie-line, the AC line voltage, AC line current amplitude, and difference of voltage phase between two sides of an AC contact line. By modifying the model parameters, the powers of transmission line between two regions are chosen as P = 150MW, P = 200MW, and P = 300MW, and thus three kinds of operation modes are derived (the positive direction of power flow is defined as from Area 1 to Area 2).

According to the procedure described in the previous section, the interarea oscillation modes are analyzed for the transmission power P = 150MW, P = 200MW, and P = 300MW, respectively, which are shown in Table 1.

By carrying out the wide-area damping controller design steps proposed in Section 3.4, the frequency domain self-excited method and the improved geometric lateral index are used to calculate the comprehensive and residue indices for different schemes. The results are shown in Tables 2–4.

As shown in Tables 2–4, the best candidate signals among the three operating modes are the rotor speed difference between G1 and G3 by comparing the comprehensive and residue indices.

In order to verify the validity of the analysis results, the wide-area damping control effect of different feedback signals

Table 2: System indices for P=150MW.

Alternative input signal	Residue index	geometric laterality index	frequency	Damping ratio	Compensation phase
the rotor speed difference of G1 and G3	0.2711	0.9409	0.5536	0.0870	93.7
the active power of the AC line	2.0689e-06	0.7241	0.5700	0.0533	147.4
AC line current amplitude	0.1376	0.8042	0.556	0.0773	16.5
difference of voltage phase between two sides of AC line	1.6235e-06	0.7171	0.567	0.0395	54.6

Table 3: System indices for P=200MW.

Alternative input signal	Residue index	geometric laterality index	frequency	Damping ratio	Compensation phase
the rotor speed difference of G1 and G3	0.3568	0.8951	0.6587	0.0473	97.2
the active power of the AC line	1.2302e-06i	0.7501	0.6331	0.0035	115.5
AC line current amplitude	0.0117	0.7276	0.6245	0.0172	31.4
difference of voltage phase between two sides of AC line	1.4371e-08	0.7330	0.5891	0.0063	29.8

Table 4: System indices for P=300MW.

Alternative input signal	Residue index	geometric laterality index	frequency	Damping ratio	Compensation phase
the rotor speed difference of G1 and G3	0.2967	0.9554	0.5572	0.0566	92.6
the active power of the AC line	6.3309e-06	0.8236	0.5401	0.0670	115.6
AC line current amplitude	0.1087	0.7183	0.5431	0.0070	55.1
difference of voltage phase between two sides of AC line	6.0653e-08	0.7496	0.5587	0.0636	165.8

is simulated by choosing the speed difference between G1 and G3 as the wide-area damping controller feedback signal, which is installed in the DC side of the main control loop. A three-phase short circuit occurred on the AC transmission line at t=10.4s, which is cleared at 10.9s. By carrying out the phase compensation method, parameters of the wide-area controller (2) can be calculated as

$$\begin{aligned} m &= 3, \\ K &= 30, \\ T_1 &= 0.02, \\ T_W &= 10, \\ \alpha &= 0.3218, \\ T_2 &= 0.5035, \\ T_3 &= 0.1620 \end{aligned} \tag{21}$$

where the operating mode corresponding to P=300MW is selected as the compensation phase of the controller parameter calculation, and let $\theta = 92.6^{\circ}$.

From Figures 4–6, it is observed that there are obvious differences in the control effect under the location of installation being selected. Considering the residue method, for the rotational speed differences of G1 and G3 as well as the

Table 5: Interarea oscillation frequency and damping ratio for system under control.

Operation mode	eigenvalue	frequency	Damping ratio
P=150MW	-0.6208+3.5014i	0.5573	0.1746
P=200MW	-0.4446+3.9169i	0.6234	0.1128
P=300MW	-0.4082+3.6602i	0.5825	0.1108

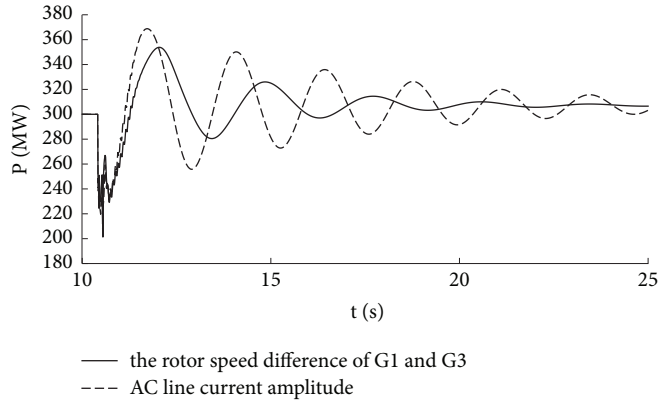

Figure 4: Comparison of power oscillation.

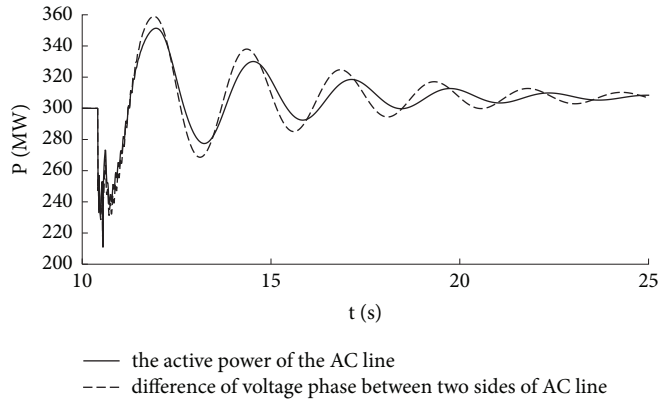

Figure 5: Comparison of power oscillation.

amplitude of the AC link current (Figure 4), the AC tie-line power P and the voltage phase difference of the tie-line (Figure 5), these two types of signals with different amplitudes are displayed as the larger the number of indicators, the better the control effect. However, since the magnitudes of the two types of signal indicators are significantly different, it is impossible to compare them at the same time. In this case, the improving geometric lateral index has a greater advantage, as it can compare different types of signals under the same order of magnitude. As shown in Figure 6, as the analysis results in Tables 2–4, the larger the index value the better the control effect, which verifies the effectiveness of the method in this paper.

For the system under wide-area damping control, the operating modes of the interarea oscillation frequency and damping ratio are calculated based on the frequency domain self-excited method as shown in Table 5.

It can be seen from Table 5 that, for system under control, the damping for each operating mode has been significantly increased, indicating that the system damping is improved under the designed controller. Simulation results of the AC tie-line transmission power with and without the designed damping controller are depicted in Figure 7. The above simulation results have verified the effectiveness and applicability of the proposed wide-area damping controller.

5. Conclusion

In this study, a wide-area damping controller design method for AC/DC hybrid power system is proposed. The input signal of the wide-area damping controller is selected by the improved geometric laterality index, which can be chosen as different types of signals to increase the range of the optional signal to improve the controller design effect. The system model can be identified through the frequency domain self-excitation method, based on which the phase compensation method is further utilized to design the DC

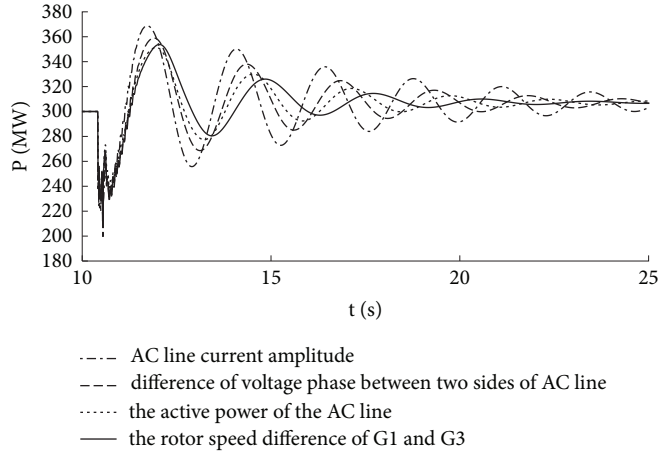

Figure 6: Active power oscillation of the tie-line.

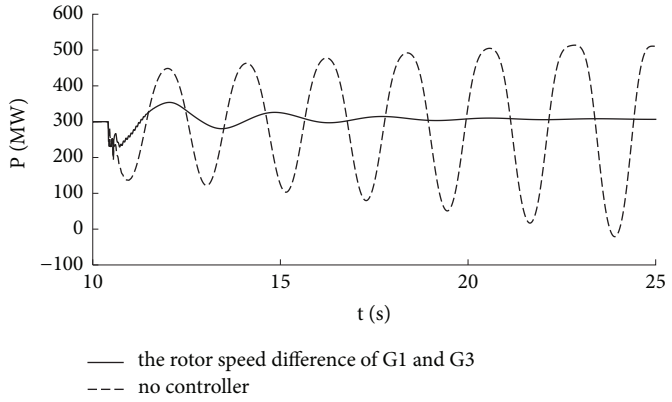

Figure 7: Transmission power comparison of the AC tie-line.

damping controller parameters. The proposed damping controller avoids the complex eigenvalue calculation in large-scale power systems and is not affected by the increase of system order. Moreover, the detailed system modeling is avoided, which may lead to inaccuracy and errors. The design process is simple, which is suitable for practical engineering applications.

Data Availability

The data used to support the findings of this study are available from the corresponding author upon request.

Conflicts of Interest

The authors declare that they have no conflicts of interest.

Acknowledgments

This research has been supported by the Young Elite Scientists Sponsorship Program by CAST (YESS20160157) and CSEE (JLB-2017-305), State Grid Corporation of China, Fundamental and Forecast Projects (XT71-18-014), and the National Natural Science Foundation of China (U1766202, 51777195) as well as the Key Project of Smart Grid Technology and Equipment of National Key Research and Development Plan of China (2016YFB0900600).

References

[1] O. F. Ruiz, I. A. DIaz DIaz, and I. Cervantes, "On the implementation of advanced hybrid controllers of AC/DC converters," *IEEE Latin America Transactions*, vol. 15, no. 9, pp. 1677–1683, 2017.

[2] A. A. Eajal, M. A. Abdelwahed, E. F. El-Saadany, and K. Ponnambalam, "A unified approach to the power flow analysis of AC/DC hybrid microgrids," *IEEE Transactions on Sustainable Energy*, vol. 7, no. 3, pp. 1145–1158, 2016.

[3] R. Jalayer and B.-T. Ooi, "Co-Ordinated PSS tuning of large power systems by combining transfer function-eigenfunction analysis (TFEA), optimization, and eigenvalue sensitivity," *IEEE Transactions on Power Systems*, vol. 29, no. 6, pp. 2672–2680, 2014.

[4] N. Rashidirad, M. Hamzeh, K. Sheshyekani, and E. Afjei, "An effective method for low-frequency oscillations damping in multiBus DC microgrids," *IEEE Journal on Emerging and Selected Topics in Circuits and Systems*, vol. 7, no. 3, pp. 403–412, 2017.

[5] S. Debnath, J. Qin, and M. Saeedifard, "Control and stability analysis of modular multilevel converter under low-frequency operation," *IEEE Transactions on Industrial Electronics*, vol. 62, no. 9, pp. 5329–5339, 2015.

[6] R. Eriksson, "A new control structure for multiterminal DC grids to damp interarea oscillations," *IEEE Transactions on Power Delivery*, vol. 31, no. 3, pp. 990–998, 2016.

[7] Y. Liu, A. Raza, K. Rouzbehi, B. Li, D. Xu, and B. W. Williams, "Dynamic resonance analysis and oscillation damping of multiterminal DC grids," *IEEE Access*, vol. 5, pp. 16974–16984, 2017.

[8] L. Meng, T. Dragicevic, J. C. Vasquez, and J. M. Guerrero, "Tertiary and secondary control levels for efficiency optimization and system damping in droop controlled DC-DC converters," *IEEE Transactions on Smart Grid*, vol. 6, no. 6, pp. 2615–2626, 2015.

[9] A. Fuchs, M. Imhof, T. Demiray, and M. Morari, "Stabilization of large power systems using vsc-hvdc and model predictive control," *IEEE Transactions on Power Delivery*, vol. 29, no. 1, pp. 480–488, 2014.

[10] J. Zhang, C. Y. Chung, C. Lu, K. Men, and L. Tu, "A novel adaptive wide area PSS based on output-only modal analysis," *IEEE Transactions on Power Systems*, vol. 30, no. 5, pp. 2633–2642, 2015.

[11] W. Yao, L. Jiang, J. Wen, Q. H. Wu, and S. Cheng, "Wide-area damping controller of Facts devices for inter-area oscillations considering communication time delays," *IEEE Transactions on Power Systems*, vol. 29, no. 1, pp. 318–329, 2014.

[12] H. N. Villegas Pico, D. C. Aliprantis, J. D. McCalley, N. Elia, and N. J. Castrillon, "Analysis of hydro-coupled power plants and design of robust control to damp oscillatory modes," *IEEE Transactions on Power Systems*, vol. 30, no. 2, pp. 632–643, 2015.

[13] R. Shah, N. Mithulananthan, K. Y. Lee, and R. C. Bansal, "Wide-area measurement signal-based stabiliser for large-scale photovoltaic plants with high variability and uncertainty," *IET Renewable Power Generation*, vol. 7, no. 6, pp. 614–622, 2013.

[14] J. M. Lim and C. L. DeMarco, "SVD-based voltage stability assessment from phasor measurement unit data," *IEEE Transactions on Power Systems*, vol. 31, no. 4, pp. 2557–2565, 2016.

[15] E. T. González and J. G. C. Guizar, "The effect of induction motor modeling in thecontext of voltage sensitivity: Combined loads and reactive power generation, on electric networks steady state analysis," *IEEE Latin America Transactions*, vol. 10, no. 4, pp. 1924–1930, 2012.

[16] D. H. A. Lee, "Voltage stability assessment using equivalent nodal analysis," *IEEE Transactions on Power Systems*, vol. 31, no. 1, pp. 454–463, 2016.

[17] A. Thangali, H. Prasad, S. Kethamakka, D. Demirdjian, and N. Checka, "AESOP: Adaptive Event detection SOftware using Programming by example," in *Proceedings of the IEEE International Symposium on Technologies for Homeland Security, HST 2015*, Waltham, Mass, USA, April 2015.

[18] P. Kundur, *Power System Stability And Control [M.S. thesis]*, McGraw-Hill Education, 1994.

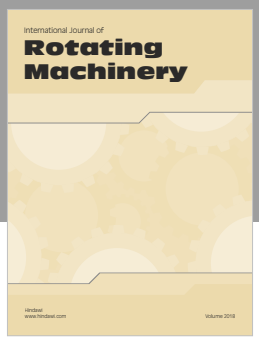

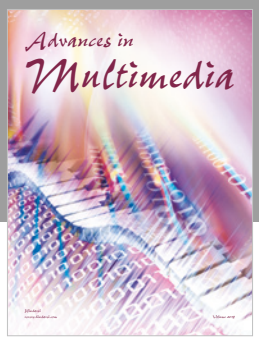

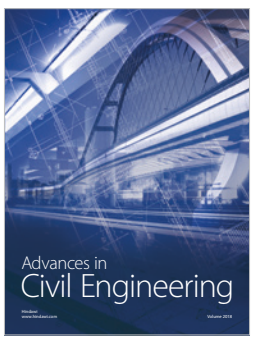

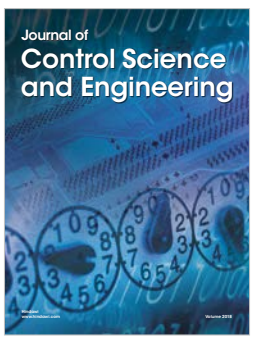

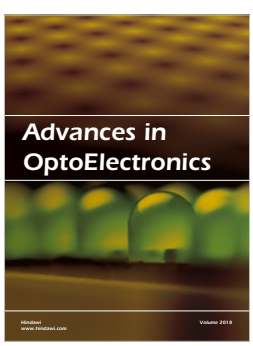

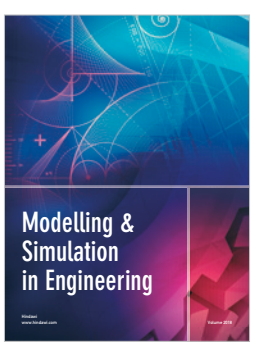

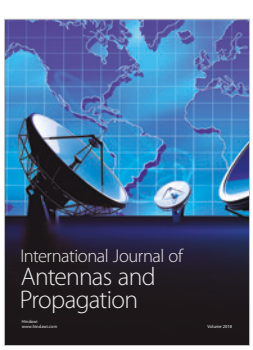

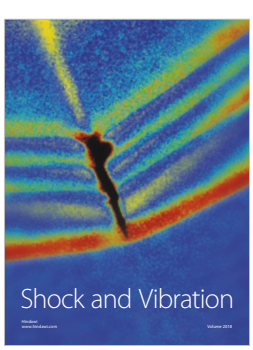

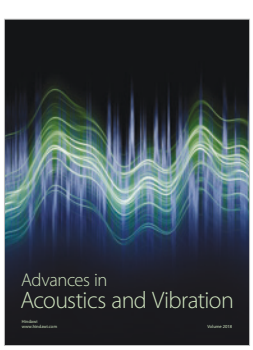

Hindawi

Submit your manuscripts at
www.hindawi.com